Leveraging Communicating UAVs for Emergency Vehicle Guidance in Urban Areas

Omar Sami Oubbati, Abderrahmane Lakas, Pascal Lorenz, Mohammed Atiquzzaman, Abbas Jamalipour

Leveraging Communicating UAVs for Emergency Vehicle Guidance in Urban Areas

Omar Sami Oubbati, *Member, IEEE,* Abderrahmane Lakas, *Member, IEEE,*
Pascal Lorenz, *Senior Member, IEEE,* Mohammed Atiquzzaman, *Senior Member, IEEE,*
Abbas Jamalipour, *Fellow, IEEE*

Abstract—The response time to emergency situations in urban areas is considered as a crucial key in limiting material damage or even saving human lives. Thanks to their "bird's eye view" and their flexible mobility, Unmanned Aerial Vehicles (UAVs) can be a promising candidate for several vital applications. Under these perspectives, we investigate the use of communicating UAVs to detect any incident on the road, provide rescue teams with their exact locations, and plot the fastest path to intervene, while considering the constraints of the roads. To efficiently inform the rescue services, a robust routing scheme is introduced to ensure a high level of communication stability based on an efficient backbone, while considering both the high mobility and the restricted energy capacity of UAVs. This allows both predicting any routing path breakage prior to its occurrence, and carrying out a balanced energy consumption among UAVs. To ensure a rapid intervention by rescue teams, UAVs communicate in an ad hoc fashion with existing vehicles on the ground to estimate the fluidity of the roads. Our system is implemented and evaluated through a series of experiments. The reported results show that each part of the system reliably succeeds in achieving its planned objective.

Index Terms—Emergency vehicle, VANET, UAV, Routing, Backbone, Search and Rescue.

1 Introduction

Everybody knows the context: you see an incident on the road and what you need to do next. It is frequently too late to locate the incident, to call the emergency, and what would be the optimal path to reach the area of interest (AoI). Indeed, people often react wrongly by firstly evaluating the collateral and material damage and then taking decisions, which can waste more time, forming a traffic jam on the way the AoI, and thus cluttered all the roads in front of rescue teams putting the lives of victims in danger.

The proliferation of Unmanned Aerial Vehicles (UAVs) in urban environments and their assistance to existing Vehicular Ad hoc Networks (VANETs) on the ground have provided a plethora of applications [1]. In fact, UAVs are extensively used in traffic monitoring [2], search and rescue missions [3], connectivity enhancement in VANETs [4], and more recently in urban surveillance [5]. The latter kind of applications is accomplished based only on multiple UAVs forming an aerial sub-network, which they can cover a wide urban area and detect any events occurred on the ground. However, without being aware of the situation on the ground, UAVs cannot achieve the planned application in an optimal way. As a solution, UAVs can communicate with ground nodes to be aware of the situation on the ground. In [6], UAVs are used to detect the isolated victim's smartphones located in a disaster area and connect them with central servers. Nevertheless, UAVs are not fully exploited neither during the search of the victims (*i.e.*, victims without smartphones) nor during the road navigation. To address these two problems, the exploitation of the UAVs' processing of captured images and their knowledge of the covered area. The work in [7] provides a 3D modeling system based on UAVs to help rescue teams to detect the victims. However, this system can be easily affected by the weather or other factors distorting the captured images. This can be addressed using sensors placed on the affected area and communicate directly with UAVs [8]. Moreover, in [9], it is supposed that UAVs have unlimited energy capacity during their deployment. Since the majority of the proposed systems and applications neglect the constraints of the restricted energy capacity of UAVs and more particularly during the exchange of messages, it is a mandatory condition to consider energy-efficient techniques.

To clearly define the use cases of our system, we consider Fig. 1 as our motivating scenario. A set of UAVs is deployed over an urban area monitoring the fluidity of the traffic and detecting any incidents on the roads. All this information is shared among UAVs in order to both have a global vision of the traffic density and what are the appropriate road segments to be traversed by the relevant services in case of incidents. Moreover, UAVs reliably inform the relevant services of any detected incidents using an energy-efficient routing protocol. This allows to facilitate the intervention of the relevant services (*e.g.*, the rescue teams if it was a traffic accident) by reaching quickly the AoI. In this paper, we have divided our system into four main parts as follows:

- *O. S. Oubbati is with the Computer Science and mathematics Laboratory, University of Laghouat, BP 37G, Ghardaïa Road, Laghouat 03000, Algeria. E-mail: s.oubbati@lagh-univ.dz.*
- *A. Lakas is with College of Information Technology, United Arab Emirates University, United Arab Emirates. E-mail: alakas@uaeu.ac.ae.*
- *P. Lorenz is with University of Haute Alsace, France. E-mail: pascal.lorenz@uha.fr.*
- *M. Atiquzzaman is with the University of Oklahoma, Norman, OK USA. E-mail: atiq@ou.edu.*
- *A. Jamalipour is with School of Electrical and Information Engineering, University of Sydney, Camperdown NSW 2006, Australia. E-mail: a.jamalipour@ieee.org.*

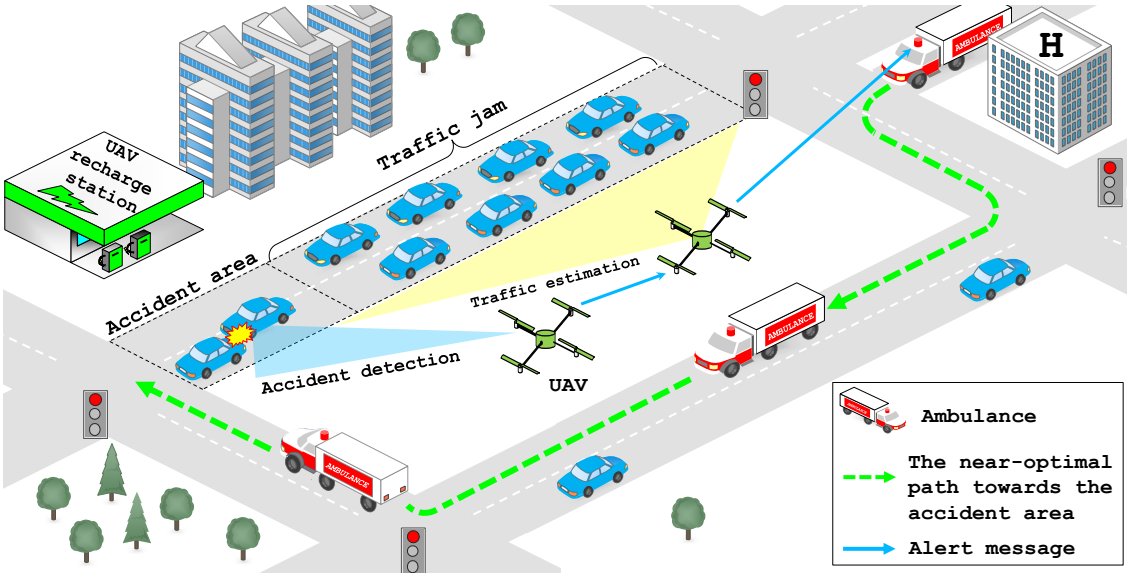

Fig. 1: Motivating scenario.

- The weighting of the road segments based on their fluidity of traffic.
- Network organization is performed to set up a permanent and robust backbone among UAVs following an energy-saving technique and connectivity measurements.
- A reactive routing is deployed only on the created backbone to establish a communication between the AoI and the relevant service.
- The calculation of the near-optimal path in terms of traveling time towards the AoI.

The rest of the paper is organized as follows. We review the most relevant and recent related work in Section 2. In Section 3, we present the system model and the method of traffic calculation. In Section 4, we investigate the organization of UAVs and how the exchange of data is structured. The performance evaluation of the system is provided in Section 5, and Section 6 draws conclusions for this work.

2 Related Work

UAV assistance for urban surveillance and rescue missions still remains a topical issue. Indeed, a team of UAVs can provide assistance to the rescue teams in real-time and perform stable communications in order to complete the mission faster. In [12], UAVs are deployed in a specified area and tried to scan and detect any beacons emitted from the missing persons' smartphones. This allows to accurately locate any missing person based on the GPS position. However, not all victims have a smartphone or can keep their smartphones during an incident, which calls this technique into question. To overcome this limitation, there are multi-agent cooperative searching, acquisition, and tracking techniques that can be adopted [18]. In [19], a path-planning algorithm is proposed to guide UAVs and tracking ground targets in rescue missions. Nevertheless, this approach does not consider the limited energy capacity of UAVs. The work in [14] adopted UAVs as LoRaWAN gateways for urban monitoring. To communicate, three factors are considered, such as the area of stress (i.e., UAVs are deployed in highly dense areas), the resilience factor, and the energy consumption factor. As a drawback, this work uses different core components with additional features, thus making the network more complex. In [15], different studies about the deployment of delay tolerant network (DTN) routing protocols in disaster areas during the communications between rescue teams and command center of search and rescue missions. Nevertheless, this kind of protocols uses the technique of store-carry and forward (SCF) that is not suitable for urgent cases, and most particularly when it comes to human life to rescue. In [16], a rapid data delivery mechanism is adopted, where the graph modeling, the dynamic programming, and the use of a tabu list are all considered to calculate the optimal routing of UAVs. But, no technique of energy conservation is proposed, and especially when the optimal routing path comprises UAVs having a low residual energy. In [20], a DTN routing protocol is proposed adopting two routing strategies according to the situation of the network. However, this protocol does not take into account the battery level of UAVs and it can fail when the next hop has a low residual energy.

UAVs can also form a substitutional connectivity solution in the sky instead of damaged infrastructures on the ground. In [10], an efficient technique is used to allow an important number of users and devices to communicate, where the data rate requirements and interference are used as key metrics to the self-adaptive power control of UAVs. Moreover, a routing protocol based on the greedy forwarding with the same behavior as in [21] is adopted, which suffers from a local optimum problem. A similar technique is used in [11], where the localization of UAVs is optimized to enhance the throughput over the covered area, while neglecting the energy constraint of UAVs. The authors in [13] combine Wireless Sensor Networks (WSNs) with UAVs in order to carry out the real-time assessment of the disaster area. But, there is any common measure adopted against the limited energy of sensors and UAVs. In the same way, the work in [17] proposes to coordinate UAVs with Unmanned

TABLE 1: Features comparison of the related applications for surveillance and rescue management.

Features	Ref. [10]	Ref. [11]	Ref. [12]	Ref. [13]	Ref. [14]	Ref. [15]	Ref. [16]	Ref. [17]	Our application
Basic ideology	UAVs assistance for 5G networks	Throughput enhancement using UAVs	Search using UAVs	UAV/WSN communication	UAVs as aerial gateways	Routing using UAVs in disaster area	UAV routing as recovery	UAV Visual assistance to USVs	Emergency vehicle guidance based on UAVs
U2G communication	√	√	√	√	√	√	√	√	√
Energy-efficiency	√	×	×	×	√	×	×	√	√
Zone awareness	×	×	×	√	√	×	×	×	√
Aerial images	√	×	×	√	×	√	×	√	√
Damage assessment	×	√	×	√	×	√	×	√	√
Incident preparedness	√	×	×	×	√	×	×	√	√
Type of area	Urban	Disaster area	Disaster area	Disaster area	Urban	Disaster area	Mountain	Sea	Urban
Ground network	All devices	Mobile	Mobile	WSN	VANET	Mobile	Mobile	USVs	VANET
Type of application	Disaster recovery	Connectivity recovery	Search	Disaster recovery	Surveillance	Connectivity recovery		Surveillance and rescue	
Routing	Geographical	—	—	Hybrid	—	Delay tolerant network	Rapid delivery	—	Energy-efficient connectivity
Major advantage	Energy-efficiency	Coverage enhancement	Targets' detection	UAV-WSN communication	Energy conservation	Efficient in sparse area	Near optimal routing	UAV-USV communication	Fastest path to the AoI
Major Limitation	Routing failure	UAVs' placement	Undetectable victims	Energy constraints	Complexity of features	Delay of delivery	Energy constraints	Human operator	UAV-vehicle communication

Surface Vehicles (USVs) to enhance the rescue missions of drowning victims. As a disadvantage, a human operator needs to be permanently present.

Our system is designated as part of search and rescue applications, which can address several features at once. Indeed, it is based on UAV-to-Ground (U2G) communication to collect beacons exchanged between vehicles forming a VANET to estimate their densities. UAV-to-UAV (U2U) communication is established relying on an energy-efficient protocol. Using its embedded digital map and GPS, our system is aware of all the zones' positions in urban roads. UAVs are permanently deployed and prepared to detect any incidents on the roads using its handling capacities of the captured images. Also, this system has the ability to plot the fastest path for rescue teams to intervene in the AoI.

TABLE 1 provides a summary of features comparison among the most relevant applications previously described, with those considered by our proposed application.

3 System Description

In a classical monitoring application exploiting the UAV-assisted vehicular network, UAVs can be considered as the efficient support to cover the area, to collect, to analyze, and to transmit crucial information about the events occurred on the ground. Our system is designed to allow UAVs to sense the surrounding road segments and monitor the variation of the traffic status. Also, UAVs coordinate between each other in terms of exchanging messages, organization, and monitoring, in order to detect any incident on the roads, reliably inform the relevant services, and facilitate their intervention. In this section, we first describe the assumptions and then present the weight calculation method for road segments by combining the traffic density and the speed of vehicles.

3.1 Assumptions

Consider a UAV system consisting of a set of n UAVs fairly dispersed in a 3 dimensional (3D) area moving randomly above the different road segments. Each UAV is initially equipped with a fully-charged battery and it is aware of both its own movement information ($i.e.$, position, speed, and velocity) and all details of the neighboring UAVs. Besides, a UAV has a state that can either be a Normal UAV or a Backbone UAV. To communicate, both UAVs and existing vehicles on the ground adopt the IEEE 802.11p wireless interfaces since they can provide a wide transmission coverage [22]. Each road segment is assumed to be divided into identified fixed zones. The size of each zone is defined based on the communication range of vehicles (≈300m). According to several simulation experiments that showed their good performances, we suppose that there is a sufficient number of UAVs where each road segment is covered by at least one UAV to increase the probability to detect any incidents on the roads.

Since, as widely known, UAVs have a limited energy capacity [23], therefore, we have defined three ratio (%) intervals of residual energy levels: (i) High energy level [66,100], (ii) Medium energy level [33,66[, and (iii) Low energy level [0,33[. It is worthy to note that UAVs have ≈300m of line of sight (LoS) range and they are hovering at a low altitude which does not exceed ≈300m. All UAVs hovering in clear weather can detect any incident on the road using its processing capabilities of the captured images, which is out of the scope of this work.

3.2 Weight calculation

To determine the weight of a road segment, the hovering UAV gathers Hello packets that are periodically exchanged between vehicles. An intercepted Hello packet comprises the movement information of the vehicle (*i.e.,* position and speed). Regardless of its energy level and state, the UAV fills and maintains a *monitoring table* of the traffic density as and when intercepting the Hello packets from all vehicles traveling on a given road segment. As shown in Fig. 2, we observe four UAVs u_1, u_2, u_3, and u_4 trying to collect the exchange of Hello packets from vehicles located on four different road segments divided into three fixed zones.

As an illustration, we take the *monitoring table* of u_3 (*see* TABLE 2) to calculate some crucial parameters which are required for the $Weight$ calculation of the segment between the two intersections I_X and I_Z.

TABLE 2: Monitoring table of u_3.

Zone	Vehicle (position (x,y))	Speed (m/s)
$Zone_1$	v_1 (100.00,5.00)	10
$Zone_2$	v_2 (90.00,305.00)	8
	v_3 (90.00,405.00)	8
$Zone_3$	v_4 (90.00,505.00)	8
	v_5 (100.00,610.00)	14
Total number of vehicles $T(S_{I_X,I_Z})$ = 5		Average speed SP_{av} = 9.6 m/s

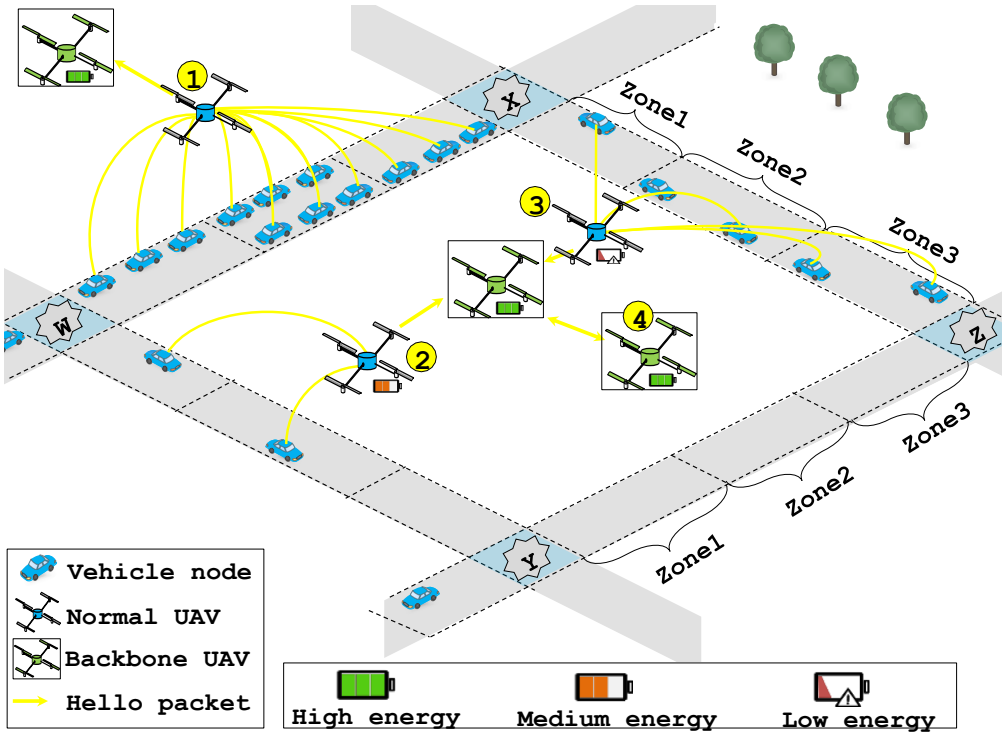

Fig. 2: Weight calculation for each road segment.

From TABLE 2 and as a generalization, we can easily deduct the well-regulation of the traffic density by calculating the standard deviation which shows how vehicles are fairly distributed in a given road segment:

$$\sigma = \sqrt{\frac{1}{|S_{I_i,I_j}|} \times \sum_{i=1}^{|S_{I_i,I_j}|} (T(Zone_i) - \mu)^2} \quad (1)$$

where,

$$T(S_{I_i,I_j}) = \sum_{i=1}^{|S_{I_i,I_j}|} T(Zone_i)$$

$$\mu = \frac{1}{|S_{I_i,I_j}|} \times \sum_{i=1}^{|S_{I_i,I_j}|} T(Zone_i)$$

$T(S_{I_i,I_j})$ is the total number of vehicles in the road segment S_{I_i,I_j} delimited by intersections I_i and I_j. μ is the average number of vehicles per zone, $T(Zone_i)$ is the number of vehicles in the zone $Zone_i$, and $|S_{I_i,I_j}|$ is the number of fixed zones within a specific road segment S_{I_i,I_j}. If for example $\sigma \approx 0$, it means that vehicles a fairly dispersed or, in a general case, they are moving, or this segment is almost empty of vehicles, which are the suitable scenarios. Otherwise (*i.e.*, $\sigma > 0$), it means that vehicles constitute nearly isolated clusters (*e.g.*, at red lights), which is the inappropriate scenario.

Based on the aforementioned metrics, a multi-criteria $Weight$ can be calculated for S_{I_i,I_j} as follows:

$$Weight = \left(\frac{T(S_{I_i,I_j})}{\sigma + 1}\right) \times \left(\frac{d(I_i, I_j)}{(SP_{av} \times 1(s)) + 1}\right) \quad (2)$$

where, $d(I_i, I_j)$ is the length of the road segment S_{I_i,I_j}.

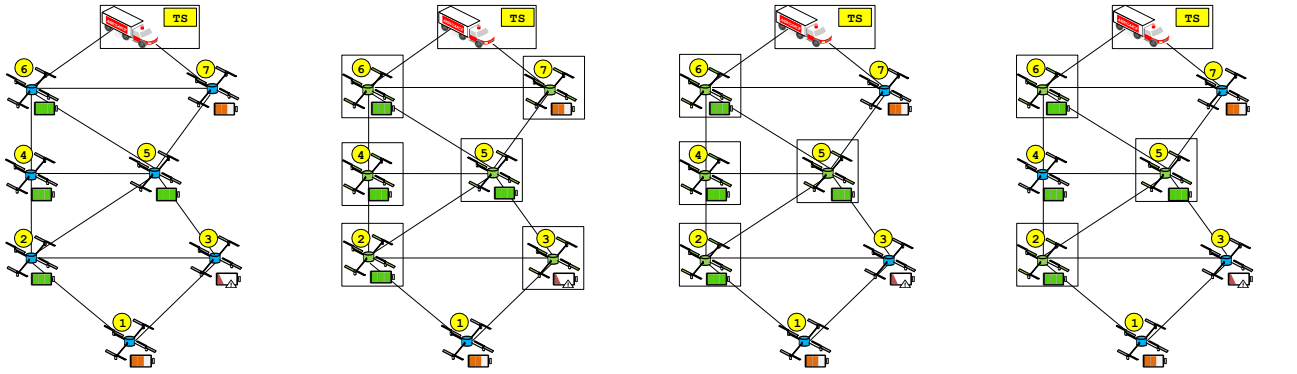

(a) Initial network. (b) CDS. (c) Energy-based CDS. (d) Connectivity-based CDS.

Fig. 3: Connected dominating set (CDS) formation.

SP_{av} is the average of vehicles' speeds in the road segment. In order to get Weight with no dimension, SP_{av} is multiplied by the factor "1(s)". $Weight$ has a proportional relationship with $T(S_{I_i,I_j})$ and $d(I_i, I_j)$. As we can observe, formula (2) is an empirical equation to compute Weight, which is a scalar that grows only in the positive side (*i.e.,* $Weight \geq 0$) and taking into account those four parameters impacting the fluidity degree of a given road segment. The less $Weight$, the better is the road segment and vice versa. All the calculated weights are included into the Hello packets and they are shared with the adjacent backbone UAVs.

To exemplify the $Weight$ calculation, we consider the scenario of Fig. 2. The different calculated metrics combining the $Weight$ are described in TABLE 3.

TABLE 3: Weight calculation scenario.

Segments	$d(I_i, I_j)$	$T(S_{I_i,I_j})$	SP_{av}	σ	$Weight$
S_{I_X,I_Z}	1500m	5	10 m/s	0.47	463.82
S_{I_Z,I_Y}	1500m	0	0 m/s	0	0.00
S_{I_Y,I_W}	1500m	2	14 m/s	0.47	136.05
S_{I_W,I_X}	1500m	12	0 m/s	1.41	7468.87

S_{I_Z,I_Y} obtains the best $Weight$ and could be selected as a road segment to be traversed by the emergency vehicle.

4 Organization and Data Routing

It is a challenging task to establish stable and reliable data delivery paths relaying alert messages while incorporating a maintenance strategy in the case of disconnections. To achieve this goal, a stable backbone is built by considering both the connectivity degree between UAVs and their residual energy. Similar works, such as [24], [25] have been proposed across the literature with the aim to form a stable backbone. However, they are mostly dedicated to low dynamic networks and cannot be adapted to a network comprising nodes with high mobility, such as UAVs.

Modeling a network as a graph provides facilities to use a set of well-known algorithms in graph-theories to build a robust backbone. In this work, we assume that UAVs, as well as the different target services (*i.e.,* destinations), are modeled as an undirected graph $G(V, E)$. V is a set of vertices (*i.e.,* UAVs and services) and E is a set of undirected edges (*i.e.,* bidirectional links between vertices existing at time t). In the subsequent discussion, we use terms vertex, UAV, and node interchangeably.

4.1 Connected dominating set formation

A *connected dominating set* or CDS is a subset $D \subseteq V$ such that every node not in D is joined to at least one node of D by some edge. Furthermore, there exists at least a path $P = \{e_i, e_a, e_b, \ldots, e_n, e_j\}$ between any pair of nodes $i, j \in D$, where $a, b, \ldots, n \in D$. To illustrate the creation of the subset D, we refer to Fig. 3. First, each UAV periodically exchanges Hello packets containing the additional fields shown in Fig. 4.

The ID field represents the UAV identifier, RE is its remaining energy, *Movement information* is its mobility details (*i.e.,* position, speed, and velocity). Each receiving node can use the information included in the *Movement information* field together with its own mobility details to calculate the connectivity-lifetime of the link between its neighbors. *List of neighbors* is its neighboring nodes. $Segments$ are the surrounding road segments in range with their corresponding weights, and $Flag$ is a bit to indicate the state of the UAV. If the UAV does not belong to the backbone $Flag = 0$, otherwise $Flag = 1$.

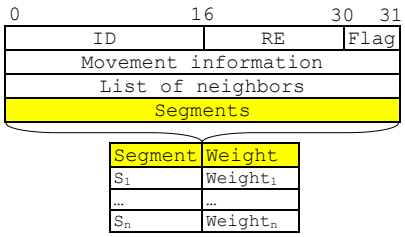

Fig. 4: Hello packet format.

To designate the backbone of UAVs or CDS, a marking process is used to mark every UAV in the connected network. $m(u_i)$ is a marker for vertex $u_i \in V$, where $m(u_i) = T$ or $m(u_i) = F$ signifying marked or unmarked, respectively. Initially, we suppose that all UAVs are unmarked, except for the $Target\ service$ (TS) which is permanently marked (or framed in Fig. 3(a)) and it belongs to the CDS. $N(u_i) = \{u_j | \{u_i, u_j\} \in E\}$ represents the neighbors of vertex u_i, *i.e.,* $u_i \notin N(u_i)$. Three steps are required for the marking process:

1) A marker F is assigned to every $u_i \in V$.
2) Every u_i exchanges its $N(u_i)$ with all its neighbors.
3) A marker T is assigned to every u_i having two unconnected neighbors.

In the example of Fig. 3(b), $N(u_1) = \{u_2, u_3\}$, $N(u_2) = \{u_1, u_3, u_4, u_5\}$, $N(u_3) = \{u_1, u_2, u_5\}$, $N(u_4) = \{u_2, u_5, u_6\}$, $N(u_5) = \{u_2, u_3, u_4, u_6, u_7\}$, $N(u_6) = \{u_4, u_5, u_7, TS\}$, and $N(u_7) = \{u_5, u_6, TS\}$. At the second step of the marking process, u_1 has $N(u_2)$ and $N(u_3)$, u_2 has $N(u_1)$, $N(u_3)$, $N(u_4)$, and $N(u_5)$, u_3 has $N(u_1)$, $N(u_2)$, and $N(u_5)$, u_4 has $N(u_2)$, $N(u_5)$, and $N(u_6)$, u_5 has $N(u_2)$, $N(u_3)$, $N(u_4)$, $N(u_6)$, and $N(u_7)$, u_6 has $N(u_4)$, $N(u_5)$, and $N(u_7)$, u_7 has $N(u_5)$ and $N(u_6)$. By applying the last step of the process, u_2, u_3, u_4, u_5, u_6, and u_7 are marked T.

As a result of the marking process, UAVs that are marked T form a subset D, where $D = \{u_i | u_i \in V, m(u_i) = T\}$. This form a subgraph M of G, where $M = G[D]$. Two desirable properties are distinguished from the induced graph M.

Property 1. *The subset D forms a dominating set of G.*
Property 2. *M is a connected subgraph.*

From Fig. 3(b), we distinguish that the majority of UAVs are forming the CDS. Consequently, the established CDS is non-minimum and it has to be reduced, since the problem of minimizing a CDS is NP-complete. To reduce $|D|$, we propose two rules based on the residual energy of each UAV and the connectivity degree between UAVs.

Rule 1. *If* $N[u_i] \subseteq N[u_j]$ *and* $RE_{u_i} < RE_{u_j}$, $m(u_i) = F$.

Where $u_i, u_j \in M$. $N[u_i] = N(u_i) \bigcup u_i$ which is called the closed neighbors of u_i. RE_{u_i} is the residual energy of u_i. When the closed neighbors of u_i are covered by those of u_j, u_i can be removed from M if $RE_{u_i} < RE_{u_j}$. It is not difficult to prove that $M - \{u_i\}$ is still a CDS of G. The condition

$N[u_i] \subseteq N[u_j]$ means that $u_i, u_j \in D$ are connected. Therefore, Properties 1 and 2 are still preserved after applying Rule 1.

In Fig. 3(c), since $N[u_7] \subseteq N[u_6]$ and $RE_{u_7} < RE_{u_6}$, node u_7 is removed from M. Node u_3 is also removed from M, since it is observed that $N[u_3] \subseteq N[u_2]$ and $RE_{u_3} < RE_{u_2}$.

Rule 2. *If* $N[u_i] \subseteq N[u_j]$ *and* $ACL_{u_i} < ACL_{u_j}$, $m(u_i) = F$.

ACL_{u_i} represents the average connectivity-lifetime between u_i and $N(u_i)$. Let $CL_{u_i,N(u_i)} = \{CL_{u_i,u_1}, CL_{u_i,u_2}, \ldots, CL_{u_i,u_j}\}$ be the set of the estimated connectivity-lifetimes between u_i and its neighbors $N(u_i)$. The average of the connectivity-lifetimes can be expressed as follows:

$$ACL_{u_i} = \frac{\sum_{j=1}^{|N(u_i)|} CL_{u_i,u_j}}{|N(u_i)|} \quad (3)$$

CL_{u_i,u_j} is the remaining time of u_i and u_j to stay connected, which can be calculated based on the method proposed in [26]. As shown in Fig. 6, let u_i and u_j be two UAVs with a LoS range of R, non zero speeds V_i and V_j, their initial locations be (X'_i, Y'_i, Z'_i) and (X'_j, Y'_j, Z'_j), and their respective velocity angles θ_i, ϕ_i and θ_j, ϕ_j.

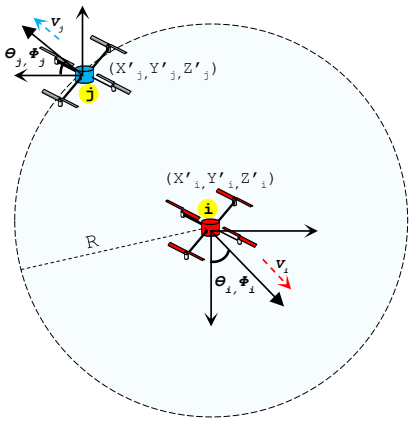

Fig. 6: Connectivity-lifetime between u_i and u_j.

The connectivity lifetime between u_i and u_j can be calculated based on the following equation:

$$CL_{u_i,u_j} = \frac{-y \pm \sqrt{y^2 - 4xz}}{2x} \quad (4)$$

where,

$$\begin{aligned} x &= w^2 + x^2 + y^2 \\ y &= 2iw + 2jx + 2oy \\ z &= m^2 + n^2 + o^2 - R^2 \\ m &= (X'_i - X'_j) \\ n &= (Y'_i - Y'_j) \\ o &= (Z'_i - Z'_j) \\ w &= (V_i \sin\theta_i \cos\phi_i - V_j \sin\theta_j \cos\phi_j) \\ x &= (V_i \sin\theta_i \cos\phi_i - V_j \sin\theta_j \cos\phi_j) \\ y &= (V_i \cos\theta_i - V_j \cos\theta_j) \end{aligned}$$

In Fig. 3(d), since $N[u_4] \subseteq N[u_5]$ and $ACL_{u_4} < ACL_{u_5}$, node u_4 is removed from M. As a result, every vertex $u_i \in M$ has a high probability of staying connected to the CDS (*i.e.,* the backbone) while ensuring a long lifetime to the backbone. It is worthy to note that the *CDS* formation is based only on the periodical exchange of Hello packets and it is automatically and permanently carried out to ensure a robust connectivity until the target services.

4.2 Routing

Once the *CDS* is determined, a novel routing strategy is deployed in any data communications between any UAVs and the relevant services. A reactive strategy is adopted while considering two factors: (i) excluding UAVs with a low residual energy level and to spare them from any data transmissions and (ii) considering the robustness of each link composing the discovered paths. To clearly highlight the novelties of our routing strategy, TABLE 4 depicts the limitations of [20] and [21] that are dedicated to UAV ad hoc networks compared with our routing strategy.

TABLE 4: Our routing strategy vs. Ref. [20] and Ref. [21]

	Our strategy	Ref. [20]	Ref. [21]
Link stability	√	×	×
Energy efficiency	√	×	×
Prediction	√	×	√
Technique	Reactive	DTN	Greedy
UAV organization	CDS	None	None
Maintenance	Alternative paths	SCF	Prediction

4.2.1 Packet format

As shown in Fig. 5(a), the route request (RREQ) packet format comprises several fields. The *Transmission ID* field identifies the discovery process to which the packet belongs. $N(S)$ is the cumulative number of segments covered by each transited UAV. $Delay_P$ is the required time for the RREQ to transit the path between the source and *TS*. *Source* and *TS* represent the identifiers of the communicating nodes. *Movement information* is the same field included into the Hello packet format depicted in Fig. 4. It allows to calculate the connectivity-lifetime between two successive nodes based on equation (4). CL_P is the connectivity lifetime of the full path, which can be defined as the lowest connectivity lifetime between any two successive nodes belonging to the path. RE_P is the residual energy ratio of the full path, which can be defined as the lowest energy level ratio in a given node belonging to the path. It is worthy to note that CL_P and RE_P are calculated progressively to the target destination. *Distance* is the number of transited UAVs.

As depicted in Fig. 5(b), the RREP packet includes the same fields as those included in the RREQ packet. These fields allow the source node to have a global knowledge of the selected path, such as its connectivity-lifetime and its residual energy. Certain values of these fields is cached in the routing tables of all the nodes constituting the path. Once the RREP packet reaches the source node, the routing path is established and the alert message comprising useful fields is ready to be sent (*c.f.,* Fig. 5(c)). The *Alert ID* corresponds to a unique identification of an incident. *Alert type* defines the kind of the incident occurred on the ground,

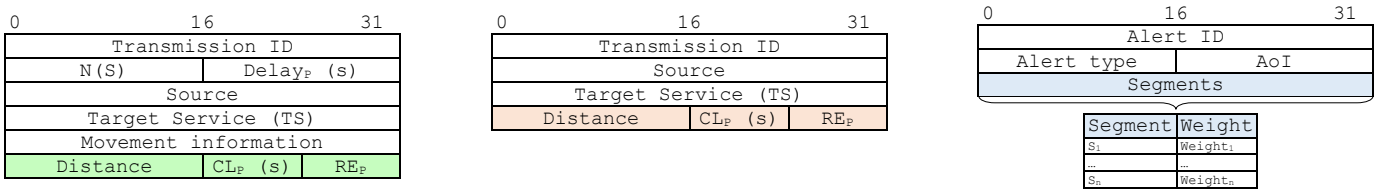

(a) An RREQ packet Format. (b) An RREP packet Format. (c) An Alert message format.

Fig. 5: Format of routing packets.

which is used to determine the appropriate target service to inform. *AoI* includes the coordinate of the exact location of the incident. As the alert message crossing the selected path to the target service, the *Segments* field accumulates the covered segments along with their corresponding weights by each transited UAV. This field is used by TS to calculate the near-optimal path on the ground towards the incident.

4.2.2 Routing process

To illustrate the discovery process, let us consider the concrete example depicted in Fig. 7. When an accident is detected on a road segment, the UAV sends immediately an alert message to the adjacent backbone UAV u_1. This message comprises useful information about the accident, such as the *Alert ID*, the *AoI*, and the *Alert type*. Initially, the *Segments* field contains the weighted road segments covered only by the UAV detecting the accident. When u_1 intercepts the *alert* message, it has to engage a data communication with the target service TS (Hospital) in order to bring back of the ambulance into the accident area. u_1 generates and broadcasts a route request (RREQ) packet to find the appropriate sequence of backbone UAVs towards TS which also belongs to the backbone. While transiting the CDS, the RREQ packet records a set of information which defines both the connectivity lifetimes and the residual energy levels of the discovered paths. To reduce the broadcast storm problem, the UAV drops the RREQ if it has already received an RREQ with the same *Transmission ID*.

Once the first RREQ is intercepted by TS, a short timer is started to collect all possible RREQs corresponding to existing routing paths. After the expiration of the timer, all RREQs are dropped and the flooding is considered to be achieved. In this case, TS has to make a routing decision to select the most connected path having a sufficient energy level. By taking into account all the calculated parameters included in the intercepted RREQs, we can define a multi-criteria score for each sequence of UAVs using the following equation:

$$Score = RE_P \times \frac{N(S)}{Distance} \times \left\lfloor \frac{CL_P}{Delay_P} \right\rfloor \quad (5)$$

From equation (5), we have the following observations:

- The floor of $\left\lfloor \frac{CL_P}{Delay_P} \right\rfloor$ is a scalar representing whether the routing path still remains connected or not during the data delivery. Therefore, it grows only on the positive side and can be equal to zero only when $CL_P < Delay_P$ or $CL_P = 0$, which means that the path can be disconnected at any time during the data delivery. However, if $\left\lfloor \frac{CE_P}{Delay_P} \right\rfloor > 0$, it means that there is a high probability that this routing path remains connected during the data transmission.
- The calculated $Score$ has a proportional relationship with RE_P and $N(S)$ which play a key role to determine the energy-efficiency of a path and its amount of information about the road segments, respectively.
- A path with a high score is suitable because it can ensure reliable data delivery while providing important global knowledge about the traffic on the road segments.

From TABLE 5, we can easily select the appropriate sequence of UAVs for alert delivery. Based on the calculated parameters included in the two intercepted RREQs, a score is calculated for $Path_1$ and $Path_2$ using the equation (5). The target TS selects $Path_1$ (*i.e.,* the sequence $u_1 \rightarrow u_2 \rightarrow u_4 \rightarrow u_5 \rightarrow TS$) since it has obtained the highest score. An RREP is generated including the calculated parameters of the selected path and it is sent back to the source u_1 through $Path_1$. During the transition of the RREP packet, a set of updates is carried out in each routing table of the transited UAVs.

TABLE 5: Discovered paths.

$Path_1$		$Path_2$	
$Delay_P = 2\ (s)$		$Delay_P = 3\ (s)$	
$CL_P = 5\ (s)$		$CL_P = 3.5\ (s)$	
$RE_P = 0.75$		$RE_P = 0.25$	
$Distance = 4$		$Distance = 5$	
$N(S)$=7		$N(S)$=6	
UAV	$N(S)$	UAV	$N(S)$
u_1	2	u_1	2
u_2	1	u_2	1
u_4	2	u_3	1
u_5	2	u_6	1
TS		u_7	1
		TS	
$Score = 2.625$		$Score = 0.3$	

Once u_1 receives the RREP packet, it adds a new entry in its routing table (*c.f.,* Fig. 8). This is crucial to start the alert transmission and maybe to send other information (*e.g.,* video recordings of the incident) in the future if the selected path is not expired. It should be stressed that all routing tables are purged after 10 (s) of inactivity, and the discovery process is a mandatory condition to make other alert transmissions. u_1, in turn, adds the road segments

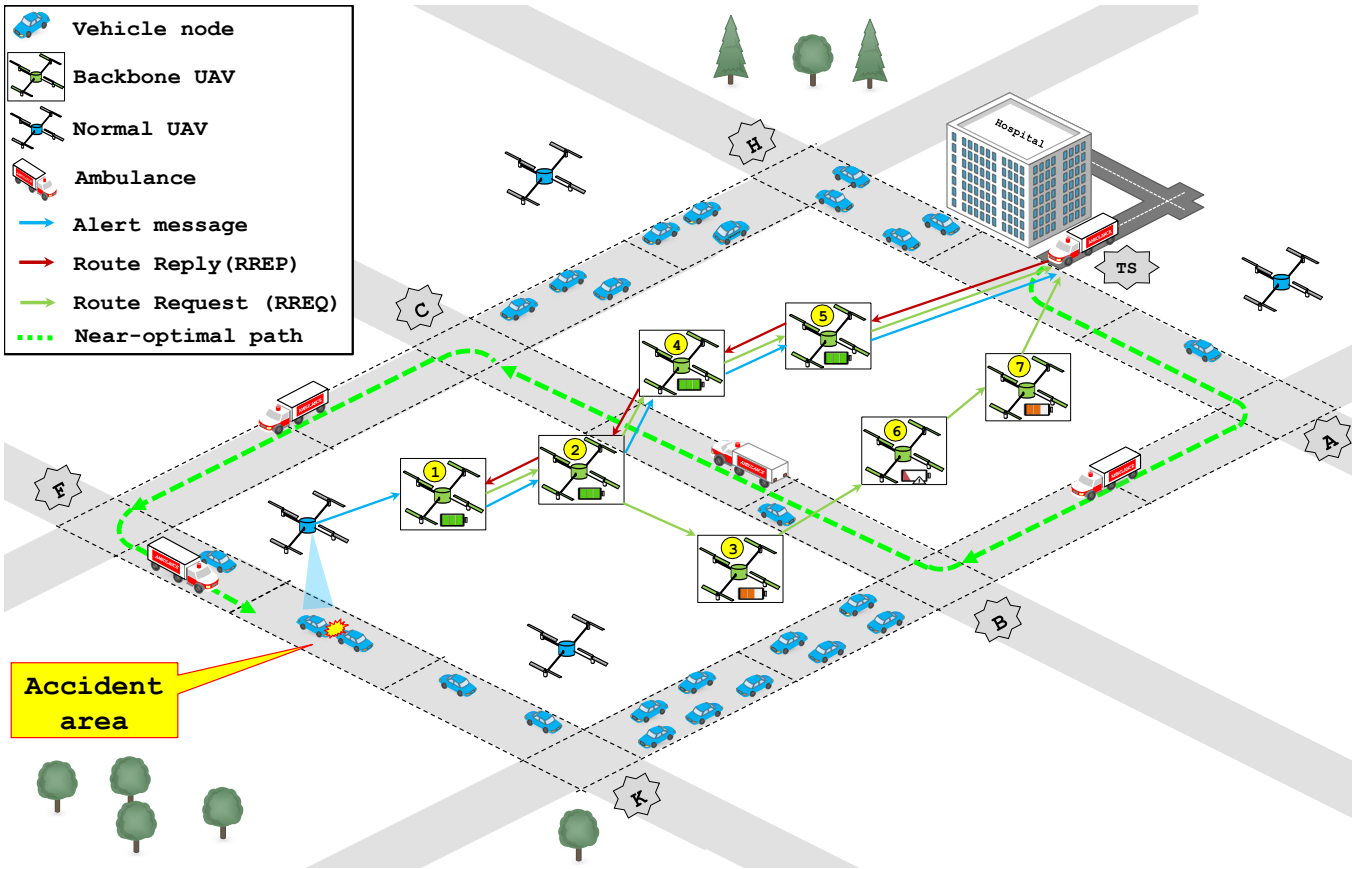

Fig. 7: Principle of our alert model functioning.

covered by itself along with their weights and it sends the *alert* message to the next hop. The same maneuver is executed by the forwarder until that the *alert* message will be delivered to the target TS.

Routing Table u_1				
Next hop	Destination	Alert ID	CL_P(s)	RE_P
u_2	TS (Hospital)	0001	5(s)	0.75
...	...	...	...	...

Fig. 8: Routing table of u_1.

When TS receives the *alert* message, it has accurate details about the incident occurred in the segment between the intersections I_F and I_K. TS has also an idea about the traffic density in the majority of the road segments in the area. TABLE 6 shows the different covered road segments along with their respective weights.

4.2.3 Near-optimal path towards the AoI

To reach the AoI (*e.g.*, accident area) in a timely manner, TS has to calculate the near-optimal path between the starting point *Ambulance* and goal *Accident area* based on the different calculated weights for road segments (*see* TABLE 6). In graph theory, the Dijkstra algorithm is highly used to find the shortest path on a road network modeled as a graph. When applying such algorithm, the cost function of a path needs to be calculated. Overall, each link (or edge) connecting two vertices on a path is weighted. Therefore,

TABLE 6: Covered road segments with their weights.

Covered area	
$N(S)$=7	
Segment	*Weight*
$S(I_{TS}, I_A)$	0.1
$S(I_{TS,I_H})$	3
$S(I_A, I_B)$	0
$S(I_B, I_K)$	7
$S(I_B, I_C)$	0.2
$S(I_C, I_H)$	5
$S(I_C, I_F)$	0
$S(I_K, I_{Accident\ area})$	2
$S(I_F, I_{Accident\ area})$	0.1

the cost function is the sum of the weights of all the edges constituting the path. Here, an edge is a road segment and its weight is the same weight calculated in Section 3.2. For instance, the cost between two nodes a and b is defined as $Cost_{a,b} = \sum_c Weight_c$, where c is the number of least weighted segments.

To illustrate the calculation of the near-optimal path, let us consider Fig. 7 which depicts a scenario of a near-optimal path calculation executed by TS. First, the road network is modeled as an undirected graph $H = (K, L)$, where K is a set of vertices (Intersections, TS, and *Accident area*) $K = \{I_A, I_B, I_C, I_H, I_F, I_K, TS, Accident\ area\}$, and L is a set of undirected edges (road segments) connecting the vertices.

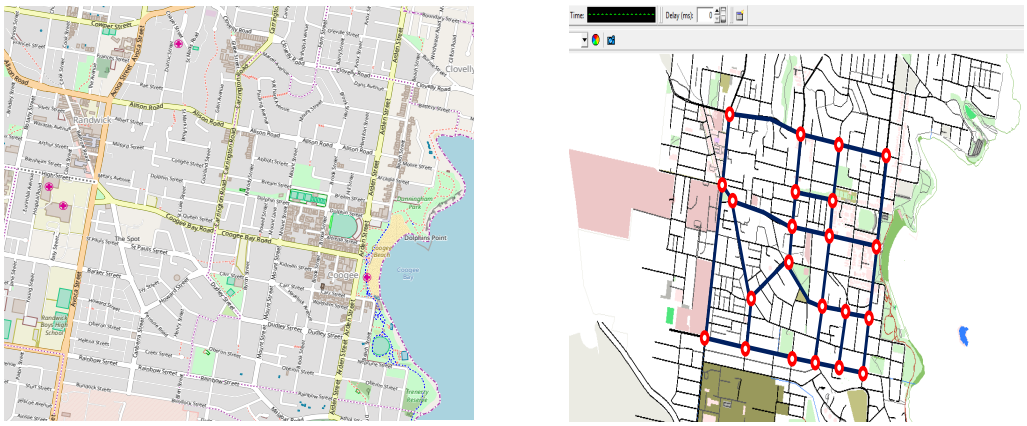

(a) Generated map. (b) Road layout.

Fig. 9: Map of the simulation area in Sydney, Australia (33°55′ 10.8″S 151°14′ 57.3″E).

By applying the Dijkstra algorithm, we obtain the following TABLE 7 which summarizes the near-optimal paths from TS towards each vertex in the road network.

TABLE 7: Shortest path calculation and costs.

Path	*Shortest path*	*Cost*
$TS \rightarrow I_A$	$TS \rightarrow I_A$	0.1
$TS \rightarrow I_H$	$TS \rightarrow I_H$	3
$TS \rightarrow I_B$	$TS \rightarrow I_A \rightarrow I_B$	0.1
$TS \rightarrow I_C$	$TS \rightarrow I_A \rightarrow I_B \rightarrow I_C$	0.3
$TS \rightarrow I_F$	$TS \rightarrow I_A \rightarrow I_B \rightarrow I_C \rightarrow I_F$	0.3
$TS \rightarrow I_K$	$TS \rightarrow I_A \rightarrow I_B \rightarrow I_C \rightarrow I_F \rightarrow I_K$	2.4
$TS \rightarrow Accident\ area$	$TS \rightarrow I_A \rightarrow I_B \rightarrow I_C \rightarrow I_F \rightarrow Accident\ area$	0.3

Based on TABLE 7, the *Ambulance* can quickly reach its target destination by following the shortest path obtained as $TS \rightarrow I_A \rightarrow I_B \rightarrow I_C \rightarrow I_F \rightarrow Accident\ area$. The cost of this path is 0.3, which can be updated on a real-time according to the traffic variation.

TABLE 8: Simulation parameters

	Parameter	Value
PHY & MAC	Frequency Band	5.9 GHz
	Transmit power	21.5 dBm
	Sensitivity	-81.5 dBm
	Path loss model	Free-space
	MAC layer	IEEE 802.11p
	Data rate	1 Mbit/s
Scenario	Area size	$3 \times 3\ km^2$
	Simulation time	300 s
	Number of UAVs	[10, 100]
	Number of vehicles	100
	Ambulance speed v_{max}	17m/s
	UAV speed v_{max}	20m/s
	UAV altitude	300m
	vehicle speed v_{max}	14m/s
Routing	Communication range of UAVs	$\approx$ 300
	Hello interval	0.1 (s)
	Data size	1 KB
	Number of accidents (senders)	20
	Initial energy of UAVs	2000 J

5 Performance Evaluation

A set of experiments is conducted to evaluate the performance of our application. We considered NS-2 that is complemented by SUMO [27] and MobiSim [28] as two mobility generators producing the movements of vehicles and UAVs, respectively. A test urban area stretched over $3 \times 3\ km^2$ is imported from OpenStreetMap [29], which knows a flexible and perpetual movement of vehicles (*c.f.* Fig. 9(a)). In the selected area, the relevant road segments and intersections are marked as blue lines and red circles (*c.f.* Fig. 9(b)). The rest of the simulation parameters are summarized in TABLE 8.

Despite its unsuitability for UAVs, a Random Way Point (RWP) mobility model is deployed for up to 100 UAVs in order to study the impact of random motions on routing protocols. Both the routing tables and the list of neighbors are purged after 10 (s) of inactivity. All UAVs are fairly distributed over the network and operate at their high energy levels. Three different experiments are performed: (i) the performance of our routing protocol is evaluated and compared with relevant routing protocols, (ii) the energy consumption is studied for each routing protocol, and (iii) different outputs of our applications are analyzed.

5.1 Routing performance

Three evaluation metrics are calculated during the experiment, such as Packet Delivery Ratio (PDR), End-to-End Delay (EED), and Overhead (OH) (*c.f.*, Fig. 10). LAROD [20] and MPGR [21] adopting different routing strategies are selected to be compared with the performance outputs of our routing protocol. Twenty communications between different accident locations and TS are established. It should be stressed that each point of the obtained results represents the mean of 30 simulation runs with 95% confidence interval. In terms of PDR (*c.f.*, Figs. 10(a) and 10(d)), our routing protocol portrays an outperforming performance under different UAV densities. Compared to the other protocols, our protocol can increase PDR by more than 20 %. This is due to the efficiently employed backbone based on the connectivity of links and the energy levels of UAVs, which is fortified as the density increases. To study the EED, we calculate the average time based on the generation time of data packets and their reception time, including the discovery process time if it is required. As shown in Figs. 10(b) and 10(e), the average EED of our protocol tends to be minimized as the density of UAVs increases. This can be explained by the initial selection of the energy-rich and most connected

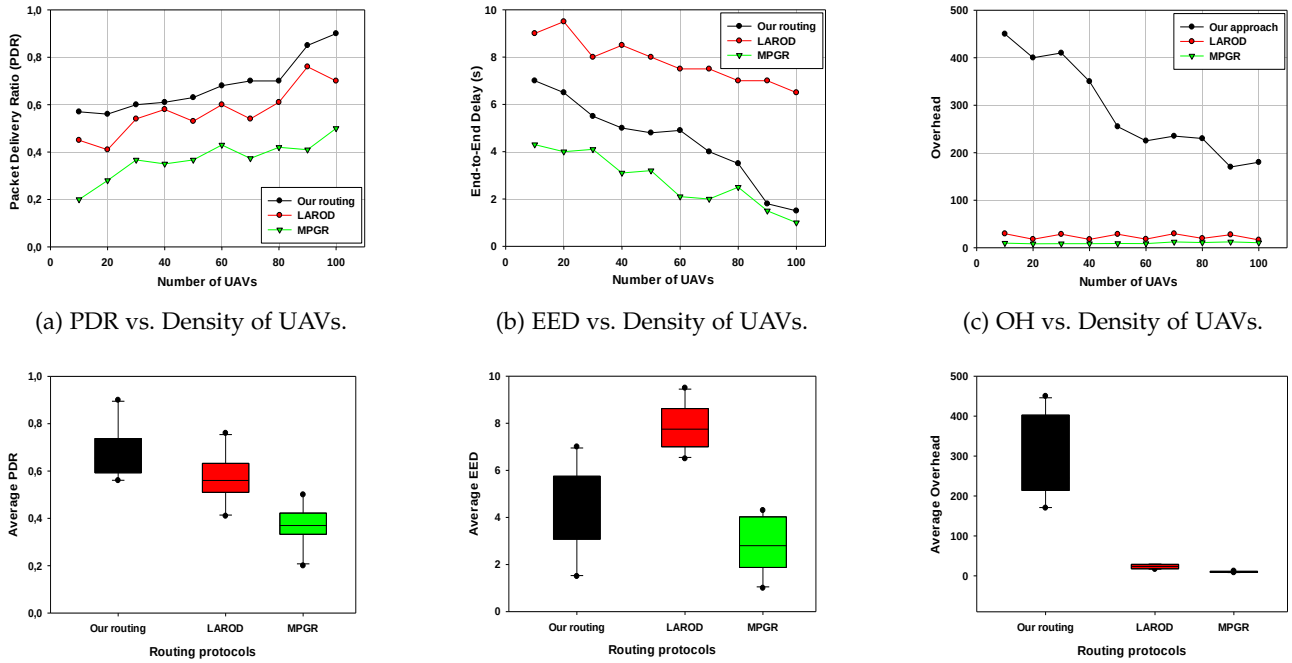

(a) PDR vs. Density of UAVs. (b) EED vs. Density of UAVs. (c) OH vs. Density of UAVs.

(d) Average PDR. (e) Average EED. (f) Average OH.

Fig. 10: Simulation results of our routing protocol vs. Density of UAVs.

routing paths remaining valid for multiple data transmission, thus gaining more time. Figs. 10(c) and 10(f) show that the control overhead required for our protocol is reduced as the density of UAVs is increasing. This is because many control packets are generated during the discovery process, and especially when the network of UAVs is poorly dense. However, the reason behind the decrease of the overhead is caused by the reduced number of route discoveries due to the long lifetime and the energy-efficient organization of the discovered paths.

5.2 Energy consumption performance

To examine the energy consumption of UAVs for all the evaluated protocols, we study the contour of the remaining energy levels of 50 UAVs at the end of each run. As a result, three graphs represented in Fig. 11, which have been smoothed based on simple interpolation.

Fig. 11(a) reveals that our protocol conducts a well-regulated energy consumption among UAVs. In essence, compared to MPGR and LAROD, our protocol relies only on backbone UAVs to transmit data packets to their corresponding destinations, where the forwarder UAVs are at their high energy levels. In addition, the backbone is permanently updated as the energy levels are under a constant variation, which will equitably distribute the transmission load among UAVs. However, we observe an important and the unbalanced energy consumption across all UAVs in MPGR and LAROD. As shown in Fig. 11(b), a very high

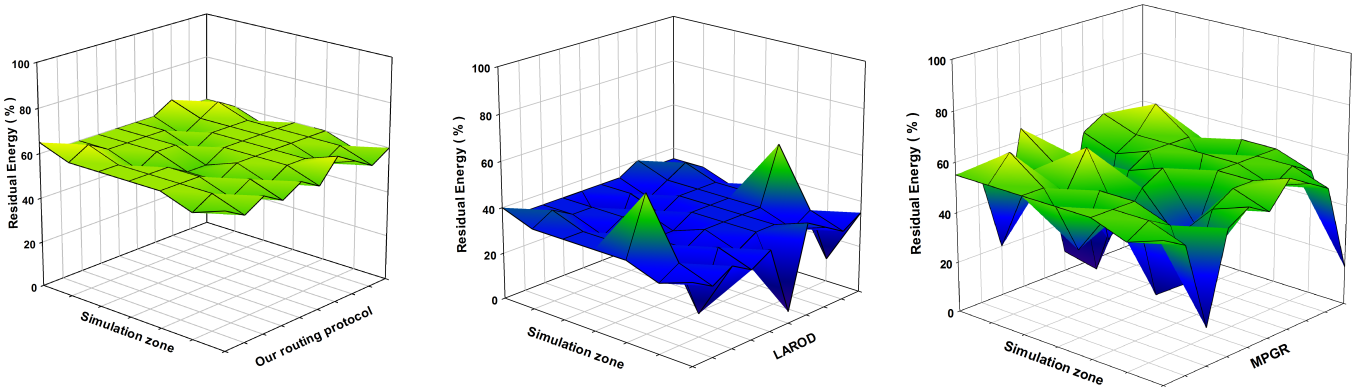

(a) RE of our routing protocol. (b) RE of LAROD. (c) RE of MPGR.

Fig. 11: Contours of residual energy levels at the end of the simulation ($UAVs = 50$).

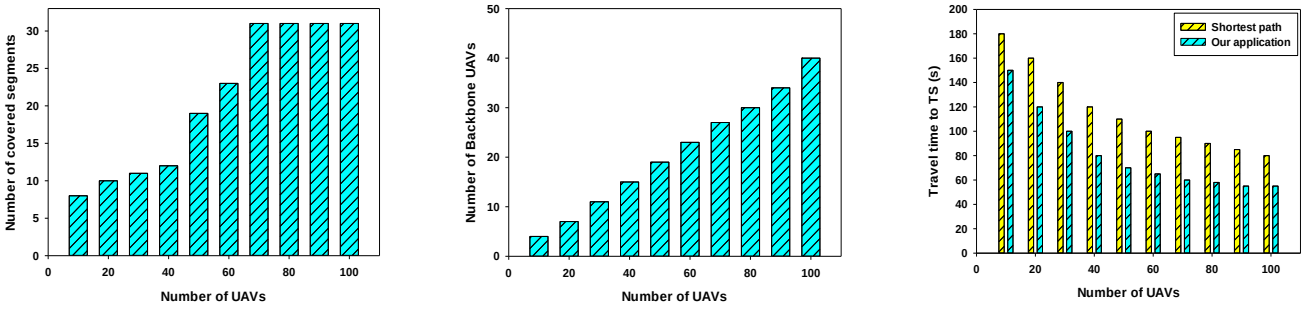

(a) Covered segments vs. Density of UAVs. (b) Backbones vs. Density of UAVs. (c) Travel time vs. Density of UAVs.

Fig. 12: Simulation results of our application.

energy consumption among UAVs that can reach up to 60%. This is due to the fact that UAVs in LAROD continue to broadcast data packets over the network if they do not overhear the broadcast of the next hops, thus consuming more energy. As for Fig. 11(c), unbalanced energy consumption is remarked, which is explained by the selection of the same chain of UAVs for the data transmissions, thus some UAVs consume more energy while others much less.

5.3 Application performance

To test the performance of our application, different experiments are performed on the road segment coverage, the number of backbone UAVs, and the travel time of the ambulance to reach the AoI.

As shown in Fig. 12(a), we deduct that the integral coverage of all road segments is reached on average at 70 UAVs. This is due to the fact that UAVs has a transmission range of 300m and the length of the road segments is a random variable, where certain segments require more than one UAV to be covered. Fig. 12(b) shows the average number of backbone UAVs according to the total density of UAVs. Indeed, we observe a uniform increase of backbone UAVs since all UAVs initially operates at their high energy levels and they are uniformly distributed over the network. As for Fig. 12(c), it is clearly shown that the average travel time taken by the ambulance through the paths provided by our application is significantly less than that achieved by the shortest path. This is explained by the fact that in the worst case, as the number of UAVs increases, our application always provides the least crowded paths, where the ambulance will cross them at its highest speed. However, the shortest paths in terms of distance can be bottled by vehicles and the ambulance has to follow them until the road empties, thus wasting more time.

6 Conclusion

As shown in the motivation scenario, the response time to emergency situations is crucial to saving human lives. Using UAVs to permanently monitor the roads, detect incidents, and inform the relevant services can help to make the rescue mission efficient and faster. With this work, we want to directly take part in the design of such systems. In fact, a weighting method is carried out in real time for all road segments hovered by the existing UAVs to measure their densities and their fluidity. This allows to have a global vision of the covered road segments and the near-optimal path to take in case of incidents. To extend the UAV network lifetime, a virtual backbone is created based on the connectedness of UAVs with a high energy level. This backbone keeps its properties by permanently updating itself according to the topology variation and the energy consumption of UAVs. In the case of an incident occurred in a given road segment, it will be detected by the UAV in charge of monitoring this segment. An alert message containing all details about the incident and the state of the roads is generated and sent through the backbone to the relevant service using an efficient routing protocol. To overcome the high mobility and the restricted energy capacity of UAVs, the deployed routing protocol exploits the discovery process to predict any link failure prior to its occurrence while achieving a regulated energy consumption. Once the relevant service gets the alert message, it calculates the near-optimal path towards the AoI. The proposed application is evaluated through a series of simulations that demonstrate its effectiveness and feasibility in real scenarios. However, we are aware of the very specific use case of our system, but we believe it can be adopted in many urban surveillance applications. Therefore, we are currently extending it to support tracking mobile objects (*e.g.,* suspect vehicles), managing traffic by controlling traffic lights, adjusting the mobility of UAVs, and taking over UAV failures. In addition, our system attempts to be a first step in this field by performing more experiments on much larger data sets, which are still needed to enhance the results achieved to date.

References

[1] O. S. Oubbati, A. Lakas, F. Zhou, M. Güneş, N. Lagraa, and M. B. Yagoubi, "Intelligent UAV-Assisted Routing Protocol for Urban VANETs," *Computer communications*, vol. 107, pp. 93–111, 2017.

[2] R. Ke, Z. Li, J. Tang, Z. Pan, and Y. Wang, "Real-Time Traffic Flow Parameter Estimation From UAV Video Based on Ensemble Classifier and Optical Flow," *IEEE Transactions on Intelligent Transportation Systems*, pp. 1–11, 2018.

[3] X. Liang, M. Zheng, and F. Zhang, "A Scalable Model-Based Learning Algorithm with Application to UAVs," *IEEE Control Systems Letters*, pp. 839–844, 2018.

[4] O. S. Oubbati, A. Lakas, F. Zhou, M. Güneş, and M. B. Yagoubi, "A survey on position-based routing protocols for Flying Ad hoc Networks (FANETs)," *Vehicular Communications*, vol. 10, pp. 29–56, 2017.
[5] V. Sharma, D. N. K. Jayakody, I. You, R. Kumar, and J. Li, "Secure and Efficient Context-Aware Localization of Drones in Urban Scenarios," *IEEE Communications Magazine*, vol. 56, no. 4, pp. 120–128, 2018.
[6] P. Li, T. Miyazaki, K. Wang, S. Guo, and W. Zhuang, "Vehicle-assist resilient information and network system for disaster management," *IEEE Transactions on Emerging Topics in Computing*, vol. 5, no. 3, pp. 438–448, 2017.
[7] S. Verykokou, A. Doulamis, G. Athanasiou, C. Ioannidis, and A. Amditis, "UAV-Based 3D modelling of disaster scenes for urban search and rescue," in *Proceedings of the IEEE International Conference on Imaging Systems and Technqiues*, 2016, pp. 106–111.
[8] M. A. Goodrich, B. S. Morse, D. Gerhardt, J. L. Cooper, M. Quigley, J. A. Adams, and C. Humphrey, "Supporting wilderness search and rescue using a camera-equipped mini UAV," *Journal of Field Robotics*, vol. 25, no. 1-2, pp. 89–110, 2008.
[9] H. Menouar, I. Guvenc, K. Akkaya, A. S. Uluagac, A. Kadri, and A. Tuncer, "UAV-enabled intelligent transportation systems for the smart city: Applications and challenges," *IEEE Communications Magazine*, vol. 55, no. 3, pp. 22–28, 2017.
[10] S. A. R. Naqvi, S. A. Hassan, H. Pervaiz, and Q. Ni, "Drone-aided communication as a key enabler for 5G and resilient public safety networks," *IEEE Communications Magazine*, vol. 56, no. 1, pp. 36–42, 2018.
[11] A. Merwaday, A. Tuncer, A. Kumbhar, and I. Guvenc, "Improved throughput coverage in natural disasters: Unmanned aerial base stations for public-safety communications," *IEEE Vehicular Technology Magazine*, vol. 11, no. 4, pp. 53–60, 2016.
[12] M. Lodeiro-Santiago, I. Santos-González, P. Caballero-Gil, and C. Caballero-Gil, "Secure system based on UAV and BLE for improving SAR missions," *Journal of Ambient Intelligence and Humanized Computing*, pp. 1–12, 2017.
[13] M. Erdelj, M. Król, and E. Natalizio, "Wireless sensor networks and multi-UAV systems for natural disaster management," *Computer Networks*, vol. 124, pp. 72–86, 2017.
[14] V. Sharma, I. You, G. Pau, M. Collotta, J. D. Lim, and J. N. Kim, "LoRaWAN-Based Energy-Efficient Surveillance by Drones for Intelligent Transportation Systems," *Energies*, vol. 11, no. 3, p. 573, 2018.
[15] J. C. de Albuquerque, S. C. de Lucena, and C. A. Campos, "Evaluating data communications in natural disaster scenarios using opportunistic networks with Unmanned Aerial Vehicles," in *Proceedings of the 19th IEEE International Conference on Intelligent Transportation Systems (ITSC)*. IEEE, 2016, pp. 1452–1457.
[16] Z. Song, H. Zhang, Y. Wang, and L. Zhang, "Unmanned Aerial Vehicles Rapid Delivery Routing of the Emergency Rescue in the Complex Mountain Region," in *Proceedings of the 13th International Conference on Computational Intelligence and Security (CIS)*. IEEE, 2017, pp. 346–349.
[17] X. Xiao, J. Dufek, T. Woodbury, and R. Murphy, "UAV assisted USV visual navigation for marine mass casualty incident response," in *Proceedings of the IEEE/RSJ International Conference on Intelligent Robots and Systems (IROS)*. IEEE, 2017, pp. 6105–6110.
[18] Y. Rizk, M. Awad, and E. W. Tunstel, "Decision making in multiagent systems: A survey," *IEEE Transactions on Cognitive and Developmental Systems*, vol. 10, no. 3, pp. 514–529, 2018.
[19] S. Ragi and E. K. Chong, "UAV path planning in a dynamic environment via partially observable Markov decision process," *IEEE Transactions on Aerospace and Electronic Systems*, vol. 49, no. 4, pp. 2397–2412, 2013.
[20] E. Kuiper and S. Nadjm-Tehrani, "Geographical routing with location service in intermittently connected MANETs," *IEEE Transactions on Vehicular Technology*, vol. 60, no. 2, pp. 592–604, 2011.
[21] L. Lin, Q. Sun, S. Wang, and F. Yang, "A geographic mobility prediction routing protocol for Ad Hoc UAV Network," in *Proceedings of the Globecom Workshops (GC Wkshps)*. IEEE, 2012, pp. 1597–1602.
[22] Z. MacHardy, A. Khan, K. Obana, and S. Iwashina, "V2X Access Technologies: Regulation, Research, and Remaining Challenges," *IEEE Communications Surveys & Tutorials*, vol. 1, no. 4, pp. 660–670, 2018.
[23] J. Wang, C. Jiang, Z. Han, Y. Ren, R. G. Maunder, and L. Hanzo, "Taking drones to the next level: Cooperative distributed unmanned-aerial-vehicular networks for small and mini drones," *IEEE Vehicular Technology Magazine*, vol. 12, no. 3, pp. 73–82, 2017.
[24] A. Kies, Z. M. Maaza, R. Belbachir, A. Boumedjout, and R. Mekki, "Routing Protocol Based on CDSE Virtual Topology in Ad Hoc Network," *Wireless Personal Communications*, vol. 80, no. 3, pp. 923–945, 2015.
[25] V. C. Sharmila and A. George, "Strategic location-based connected dominating set for mobile ad hoc networks," in *Proceedings of the International Conference on Advances in Communications, Network and Computing*. Elsevier Publications, 2014.
[26] M. Uddin *et al.*, "Link expiration time-aware routing protocol for UWSNs," *Journal of Sensors*, vol. 2013, pp. 1–9, 2013.
[27] M. Behrisch, L. Bieker, J. Erdmann, and D. Krajzewicz, "SUMO–simulation of urban mobility: an overview," in *Proceedings of the Third International Conference on Advances in System Simulation (SIMUL 2011)*, 2011.
[28] S. M. Mousavi, H. R. Rabiee, M. Moshref, and A. Dabirmoghaddam, "Mobisim: A framework for simulation of mobility models in mobile ad-hoc networks," in *Proceedings of the third IEEE International Conference on Wireless and Mobile Computing, Networking and Communications (WiMOB)*. IEEE, 2007, pp. 82–82.
[29] M. Haklay and P. Weber, "Openstreetmap: User-generated street maps," *Ieee Pervas Comput*, vol. 7, no. 4, pp. 12–18, 2008.

Omar Sami Oubbati is an Associate Professor at the Electronics departement, University of Laghouat, Algeria and a Research Assistant in the Computer Science and Mathematics Lab (LIM) at the same university. He received his degree of Engineer (2010), M.Sc. in Computer Engineering (2011), M.Sc. degree (2014), and a PhD in Computer Science (2018). From Oct. 2016 to Oct. 2017, he was a Visiting Student with the Laboratory of Computer Science, University of Avignon, France. His main research interests are in Flying and Vehicular ad hoc networks, Visible light communications, Energy efficiency and Internet of Things (IoT). He is a reviewer in many international journals and a TPC member in many international conferences. He is a member of the IEEE and IEEE Communications Society.

Abderrahmane Lakas received his MS (1990) and PhD (1996) in Computer Systems from the University of Paris VI, Paris, France. He joined the College of Information Technology, UAE University in 2003. He is teaching various courses on computer networks and network security. Dr. Lakas had many years of industrial experience holding various technical positions in telecommunication companies such as Netrake (Plano, Texas, 2002), Nortel (Ottawa, 2000) and Newbridge (Ottawa, 1998). He spent two years (94-96) as a Research Associate at the University of Lancaster, UK. Dr. Lakas has been conducting research in the areas of network design and performance, voice over IP, quality of service and wireless networks. He is a member of the IEEE and IEEE Communications Society. Dr. Lakas is in the editorial board of Journal of Communications (Actapress), and Journal of Computer Systems, Networks, and Communications (Hindawi). He is serving on the technical program committees of many international conferences GLOBCOM, ICC, VTC, etc.

Pascal Lorenz received his M.Sc. (1990) and Ph.D. (1994) from the University of Nancy, France. Between 1990 and 1995 he was a research engineer at WorldFIP Europe and at Alcatel-Alsthom. He is a professor at the University of Haute-Alsace, France, since 1995. His research interests include QoS, wireless networks and high-speed networks. He is the author/co-author of 3 books, 3 patents and 200 international publications in refereed journals and conferences. He was Technical Editor of the IEEE Communications Magazine Editorial Board (2000-2006), IEEE Networks Magazine since 2015, IEEE Transactions on Vehicular Technology since 2017, Chair of IEEE ComSoc France (2014-2018), Financial chair of IEEE France (2017-2019), Chair of Vertical Issues in Communication Systems Technical Committee Cluster (2008-2009), Chair of the Communications Systems Integration and Modeling Technical Committee (2003-2009), Chair of the Communications Software Technical Committee (2008-2010) and Chair of the Technical Committee on Information Infrastructure and Networking (2016-2017). He has served as Co-Program Chair of IEEE WCNC'2012 and ICC'2004, Executive Vice-Chair of ICC'2017, Panel sessions co-chair for Globecom'16, tutorial chair of VTC'2013 Spring and WCNC'2010, track chair of PIMRC'2012 and WCNC'2014, symposium Co-Chair at Globecom 2007-2011, ICC 2008-2010, ICC'2014 and '2016. He has served as Co-Guest Editor for special issues of IEEE Communications Magazine, Networks Magazine, Wireless Communications Magazine, Telecommunications Systems and LNCS. He is associate Editor for International Journal of Communication Systems (IJCS-Wiley), Journal on Security and Communication Networks (SCN-Wiley) and International Journal of Business Data Communications and Networking, Journal of Network and Computer Applications (JNCA-Elsevier). He is senior member of the IEEE, IARIA fellow and member of many international program committees. He has organized many conferences, chaired several technical sessions and gave tutorials at major international conferences. He was IEEE ComSoc Distinguished Lecturer Tour during 2013-2014.

Mohammed Atiquzzaman received the M.S. and Ph.D. degrees in electrical engineering and electronics from the University of Manchester, U.K., in 1984 and 1987, respectively. He currently holds the Edith J. Kinney Gaylord Presidential Professorship with the School of Computer Science, University of Oklahoma, USA. His research has been funded by the National Science Foundation, National Aeronautics and Space Administration, U.S. Air Force, Cisco, and Honeywell. He co-authored Performance of TCP/IP Over ATM Networks and has authored over 270 refereed publications. His current research interests are in areas of transport protocols, wireless and mobile networks, ad hoc networks, satellite networks, power-aware networking, and optical communications. He Co-Chaired the IEEE High Performance Switching and Routing Symposium (2003, 2011), IEEE GLOBECOM and ICC (2014, 2012, 2010, 2009, 2007, and 2006), IEEE VTC (2013), and SPIE Quality of Service Over Next Generation Data Networks conferences (2001, 2002, and 2003). He was the Panels Co-Chair of INFOCOM'05, and has been on the program committee of many conferences, such as INFOCOM, GLOBECOM, ICCCN, ICCIT, Local Computer Networks, and serves on the review panels at the National Science Foundation. He is the current Chair of the IEEE Communication Society Technical Committee on Communications Switching and Routing. He received the IEEE Communication Society's Fred W. Ellersick Prize and the NASA Group Achievement Award for outstanding work to further NASA Glenn Research Center's efforts in the area of the Advanced Communications/Air Traffic Management's Fiber Optic Signal Distribution for Aeronautical Communications project. He is the Editor-in-Chief of Journal of Networks and Computer Applications, the founding Editor-in-Chief of Vehicular Communications, and serves/served on the editorial boards of many journals, including IEEE Communications Magazine, Real Time Imaging Journal, International Journal of Communication Networks and Distributed Systems, Journal of Sensor Networks, and International Journal of Communication Systems.

Abbas Jamalipour is the Professor of Ubiquitous Mobile Networking at the University of Sydney, Australia, and holds a PhD in Electrical Engineering from Nagoya University, Japan. He is a Fellow of the Institute of Electrical and Electronics Engineers (IEEE), a Fellow of the Institute of Electrical, Information, and Communication Engineers (IEICE) and a Fellow of the Institution of Engineers Australia, an ACM Professional Member, and an IEEE Distinguished Lecturer. He is the Deputy Director for the Centre of Excellence in Telecommunications, and leads the Wireless Networking Group (WiNG) at the University of Sydney. He is the author of eight technical books, nine book chapters, and over 450 technical papers in scholarly journals and international conferences, as well as five patents, all in the area of wireless communications. He is the recipient of many prestigious awards including the 2010 IEEE ComSoc Harold Sobol Award, the 2010 Royal Academy of Engineering UK Distinguished Fellowship, the 2006 IEEE ComSoc Distinguished Contribution to Satellite Communications Award, the 2006 IEEE ComSoc Best Tutorial Paper Award, and 15 best paper awards. He was the Editor-in-Chief IEEE Wireless Communications and currently he is an editor for several scholarly journals, including IEEE Trans. on Vehicular Technology, IEEE Access, ETRI, as well as EiC of the VTS Mobile World. He has served in many IEEE positions including ComSoc Vice President for Conferences; Member ComSoc Finance Committee; Member ComSoc On-Line Contents Committee; Member ComSoc Education Board; Member ComSoc Conference Boards; Member IEEE TAB/PSPB Products & Services Committee; Chair Communication Switching and Routing TC; Chair Satellite and Space Communications TC; Vice-Director Asia Pacific Board. He has been a General Chair/Technical Program Chair/Vice Chair of major IEEE conferences (e.g., RWS'08, RWS'09, WCNC'10, GLOBECOM'10, ICC'11, GLOBECOM'12, PIMRC'12; ICC'14; ICT'15, SmartGridComm2016, GLOBECOM2018). Professor Jamalipour is an elected and voting member of the Board of Governors since 2014, and currently the Executive Vice President of the IEEE Vehicular Technology Society as well as Chair of Fellow Evaluation Committee. He is one of the most cited researchers in the field of mobile, cellular, and satellite networks with over 10 000 citations.